



Numerical Simulation Study on the Damage Characteristics of Linear Shaped Charge Jets Penetrating Rubber Targets

Zaihua Xu¹, Nan Zhou^{1*}, Ning Wang², Minhui Gu², Kui Tang², Jinxiang Wang², Yueshu Zhao¹, Qiuchen Tao¹

¹Nanjing Police University, Nanjing 210023, China

²Nanjing University of Science and Technology, Nanjing 210023, China

*Corresponding author's e-mail: nudge@163.com

Abstract. To effectively address the issue of controlled or suspected vehicles attempting to breach checkpoints after decelerating or stopping, based on a full investigation of the research status in this field, this paper proposes and designs a linear shaped charge jet perforation structure. The structure aims to disable vehicle mobility by damaging automobile tires. This paper mainly conducts a numerical study on the jet forming characteristics of the linear shaped charge jet perforation structure and its damage effect on rubber vehicle tires, and discusses the influence of the conical angle. Results indicate that the liner angle exhibits significant regular characteristics in influencing the penetration behavior of shaped charge jets into rubber targets. As the liner angle increases, the extent of rubber target damage becomes more pronounced, while the time of jet impact on the rubber target is delayed. The research presented in this paper establishes a reference foundation for studies on material structure failure mechanisms and provides technical support for equipment development.

Keywords: explosive mechanics; shaped charge liner; shaped charge jet; rubber target

1 Introduction

Vehicle-ramming terrorist acts, also known as terrorist vehicle ramming attacks, primarily refer to acts where terrorists drive or remotely operate vehicles to collide with specific targets using the vehicle body, such as government buildings, gas stations, railway/bus stations, etc., or to hijack hostages, ram into pedestrians, or run over individuals on streets. With rapid economic development, the continuous growth of motor vehicle ownership has intensified issues related to vehicle-related illegal activities, particularly major traffic violations such as drug-impaired driving, alcohol-impaired driving, speeding, and others, which severely endanger normal traffic management order and even public safety and property.

In the research of vehicle interception devices, the commonly used interception devices mainly include rigid interception devices, flexible interception devices, chemical agent devices, and their integration with intelligent interception systems. Specifically, these include setting up roadblocks, deploying tire deflation devices, and flexible vehicle-blocking nets, which mainly achieve the interception effect through methods such as blocking and road spikes [1]. However, all the above methods require pre-deployment and lack the ability to respond quickly to dangerous driving behaviors such as sudden attempts to rush through checkpoints. In order to solve the problem that the vehicle under inspection and control or the suspected vehicle attempts to ram through the checkpoint after slowing down or stopping, this paper proposes and designs a linear shaped charge jet perforation structure, which is used to damage the automobile tires, thus making the vehicle lose its mobility.

In the research on shaped charge jet penetration, extensive studies have been conducted on various aspects, including the influence of liner shape on shaped charge jet formation [2,3], the hole diameter of shaped charge jet penetration into different target plates [4], the detonation capability of shaped charge jets with different charge diameters [5,6], the penetration depth of shaped charge jets [7], and the penetration and damage effects of shaped charge jets on different material structures [8-10]. In terms of numerical calculations, the current research generally employs finite element software (such as ANSYS/LS-DYNA) to conduct numerical simulations of the penetration process of shaped charge jets, and the reliability of the models is verified through experiments [11,12]. This indicates that the application of numerical simulation methods in the field of shaped charge jets has become relatively mature. However, further exploration is still needed for the dynamic response simulation of high-elasticity materials such as rubber targets.

This paper mainly conducts a numerical study on the jet forming characteristics of the linear shaped charge jet perforation structure and its damage effect on rubber vehicle tires, and discusses the influence of the conical angle. Through the research work carried out in this paper, it can effectively solve the problem that the vehicle under inspection and control or the suspected vehicle attempts to ram through the checkpoint after slowing down or stopping. The research provides a reference basis for the study of material structure failure and offers technical support for equipment development.

2 Numerical Simulation

To comprehensively analyze the formation and penetration damage process of shaped charge jets, the numerical simulation of the jet formation process of linear liner structures with different conical angles and their penetration effects on rubber targets was conducted using the ANSYS/LS-DYNA simulation analysis software.

2.1 Model Establishment

The finite element calculation model mainly includes explosive, explosive liner, shell, air, and rubber target. A three-dimensional calculation model is adopted, and the SALE

(Structured Arbitrary Lagrangian-Eulerian) algorithm is used as the calculation algorithm. The Lagrangian grid size is divided according to 0.025 cm, and the grid division size of the SALE domain is also 0.025 cm. The calculation units are in cm-g-μs (centimeters, grams, microseconds). The height of the explosive charge is 2 cm, the width is 1.6 cm, and the linear length is 6 cm. The length of the explosive liner is 5 cm, and the thickness is 0.1 cm. The conical angles of the explosive liner are set to 60°, 90°, and 120° respectively. The size of the rubber target is 8 cm (length)×3 cm (width)×2.5 cm (height). Considering the symmetry of the model, in order to improve the calculation efficiency, a 1/4 calculation model is established, and the model is shown in Figure 1.

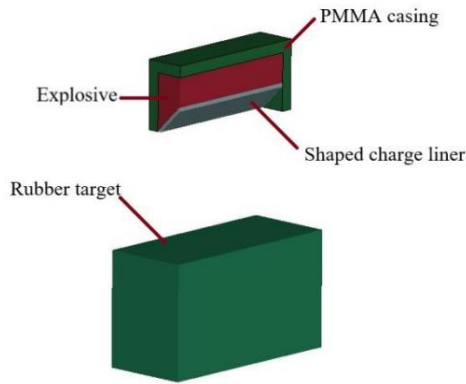


Fig. 1. A 1/4 finite element calculation model.

2.2 Material Parameters

The explosive charge is TNT explosive, the *MAT_HIGH_EXPLOSIVE_BURN model and the *EOS_JWL equation of state are adopted. The equation of state is shown in formula (1), and the parameters used are shown in Table 1 [13,14]. The material of the explosive liner is red copper, the *MAT_STEINBERG model and the *EOS_GRUNEISEN equation of state are used, as shown in formula (2), and the parameters used are shown in Table 2. The target plate is made of rubber material, and the *MAT_PIECEWISE_LINEAR_PLASTICITY model is adopted, and the parameters are shown in Table 3.

$$P = A \left(1 - \frac{\omega}{R_1 V} \right) e^{-R_1 V} + B \left(1 - \frac{\omega}{R_2 V} \right) e^{-R_2 V} + \frac{\omega E}{V} \quad (1)$$

where P is the detonation product pressure, V is the relative volume, E is the internal energy per unit volume, and A, B, R_1, R_2, ω are the JWL coefficients, which are determined by experiments.

$$G = G_0 [1 + bpV^{1/3} - h \left(\frac{E_t - E_c}{3R'} - 300 \right)] e^{\frac{-fE_i}{E_m - E_i}} \quad (2)$$

where p is pressure, V is the relative volume, E_c is the cold compression energy, and E_m is the melting energy.

Table 1. JWL parameters of TNT.

Density ρ ($\text{g}\cdot\text{cm}^{-3}$)	Detonation velocity V_D ($\text{m}\cdot\text{s}^{-1}$)	Ve - (GPa)	Pressure P_{CJ} (GPa)	A (GPa)	B (GPa)	R_1	R_2	ω
1631	6717	18.5	307	3.898	4.485	0.79	0.3	

Table 2. Model parameters of shaped charge liner.

ρ ($\text{kg}\cdot\text{m}^{-3}$)	G (GPa)	σ (GPa)	BETA	n	σ_m (GPa)	B (GPa)	B_p (GPa)	T_{m0} (K)	γ_0	S
8.93	48	0.12	36	0.45	0.64	289.3	289.3	1790	2.04	1.5

Table 3. Calculation parameters of rubber target.

ρ ($\text{kg}\cdot\text{m}^{-3}$)	E (GPa)	PR	σ_y (GPa)	EPS1 ^a	EPS2	EPS3	EPS4
1.3	2.461	0.323	0.025	0.000	0.010	0.029	0.070
EPS5	EPS6	ES1 ^b (GPa)	ES2 (GPa)	ES3 (GPa)	ES4 (GPa)	ES5 (GPa)	ES6 (GPa)
0.400	1.000	0.000	0.025	0.030	0.033	0.036	0.030

^a EPS1-6: Effective plastic strain values, at least two points should be defined.

^b ES1-6: Yield stress values.

3 Results and Analysis

To comprehensively analyze the formation and penetration damage process of shaped charge jets, based on the results of numerical simulation, the jet forming characteristics of the linear shaped charge jet perforation structure and its damage effect on rubber vehicle tires have been researched, and the influence of the conical angle were discussed.

3.1 Formation of the Shaped Charge Jet and its Damage Process

During the numerical calculation process, the standoff distance was maintained consistently at 4 cm. Under the explosive detonation, the structural variation characteristics of shaped charge jets formed by liners with different cone angles and their typical damage morphologies during the failure process of rubber targets are shown in Figure 2-4 respectively, with the observation direction aligned along the length direction of the liner (i.e., the symmetry direction of the liner).

Numerical simulation studies of shaped charge jets based on nonlinear finite element methods reveal that the influence of liner angles on the penetration behavior of rubber

targets exhibits significant regular characteristics. The simulation results demonstrate that when the liner angle is 60° , the formed shaped charge jet undergoes substantial tensile fractures during the forming process. Its initial segment achieves a high peak velocity but exhibits limited effective mass. During penetration into rubber targets, the velocity decay rate increases due to viscoelastic dissipation effects. Notably, when the secondary jet interacts with the target, the primary jet experiences velocity re-acceleration caused by pressure wave reflection.

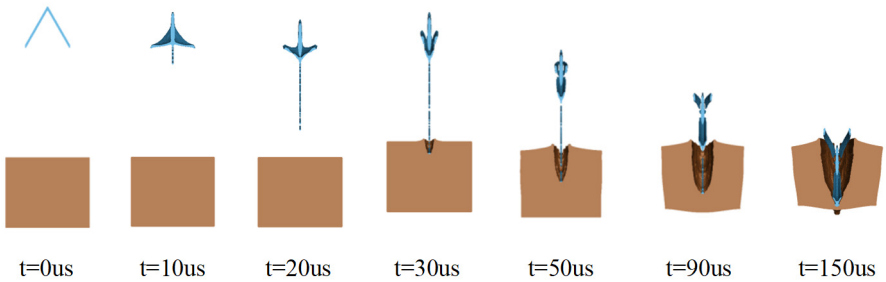


Fig. 2. Morphology of the shaped charge jet at different times and its damage to the rubber target (with a cone angle of 60°).

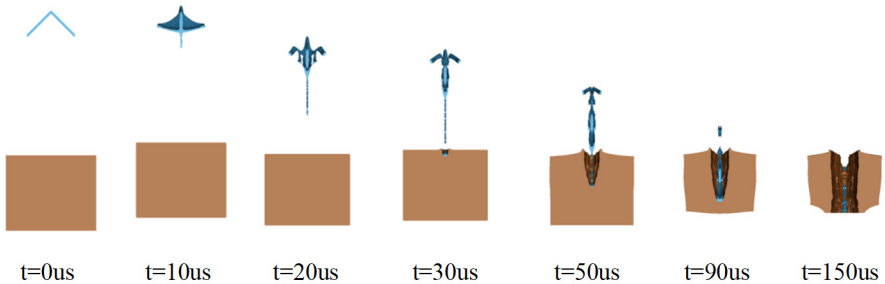


Fig. 3. Morphology of the shaped charge jet at different times and its damage to the rubber target (with a cone angle of 90°).

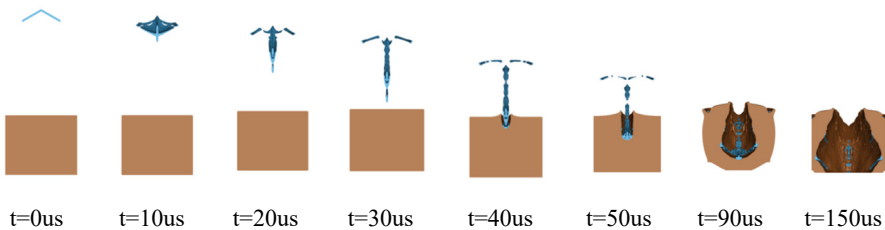


Fig. 4. Morphology of the shaped charge jet at different times and its damage to the rubber target (with a cone angle of 120°).

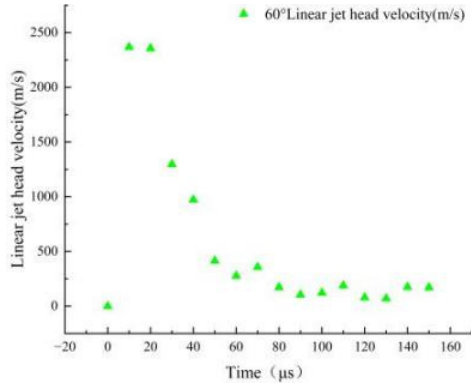
Comparative analysis indicates that when the liner angle is 90° , the formed jet exhibits fewer tensile fractures compared to the 60° configuration, though its jet head maintains similar velocity gradient characteristics. When the liner angle reaches 120° , the jet displays the most ideal continuity in morphology (with minimal fracture points) among the three angles, yet its maximum velocity value decreases compared to the 60° liner structure.

Furthermore, the final damage patterns of the rubber targets reveal significant differences in both the shape and dimensions of destruction when liners with varying conical angles are employed. For liner angles of 60° and 90° , although the morphologies of the shaped charge jets differ, both the interaction duration between the jets and the rubber targets, as well as the final expanded hole diameters in the targets, remain largely consistent. However, when the liner angle increases to 120° , the jet arrival time to the rubber target is delayed by approximately $10 \mu\text{s}$, and the target exhibits pronounced cavitation damage with a cavity diameter notably larger than those observed in the previous cases. These findings demonstrate that as the conical angle increases, the time for the shaped charge jet to act on the rubber target gradually extends, while the severity of target damage progressively intensifies.

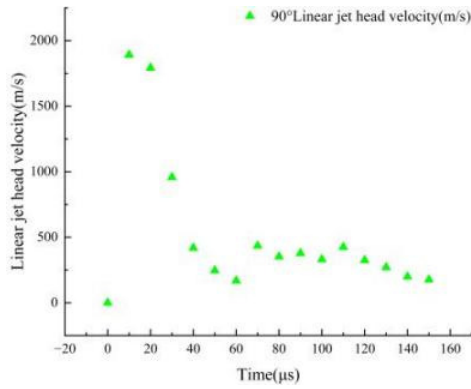
3.2 Velocity Distribution Characteristics of the Shaped Charge Jet Head

The temporal variation of shaped charge jet head velocity under different cone angles is presented in Figure 5. The figure illustrates the scatter distribution characteristics of jet head velocity at representative times, while the velocity-time fitting curves of shaped charge jet heads under different cone angles are shown in Figure 6.

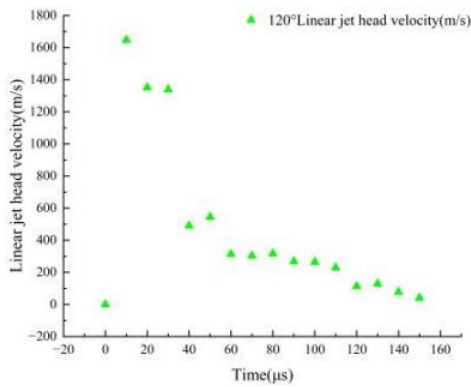
From the scatter plots of jet head velocity at different times (Figure 5), it can be observed that during the jet formation stage, the head velocity rapidly reaches its maximum within $10 \mu\text{s}$, with consistent upward trends across all three angles. In the velocity decline stage, distinct velocity distribution patterns emerge due to differences in the formation and fracture modes of different projectile structures. Further analysis of the velocity fitting curves (Figure 6) reveals that during the jet development phase, the maximum head velocity decreases inversely with increasing liner cone angle, with a velocity difference of up to 1000m/s between the maximum and minimum values. After the shaped charge jet impacts the rubber target, the head velocity drops sharply, with the velocity decay rate gradually stabilizing and approaching zero in the later stage, demonstrating consistent variation trends across all three angles.



cone angle = 60°



cone angle = 90°



cone angle = 120°

Fig. 5. Scatter plots of jet head velocity at different times.

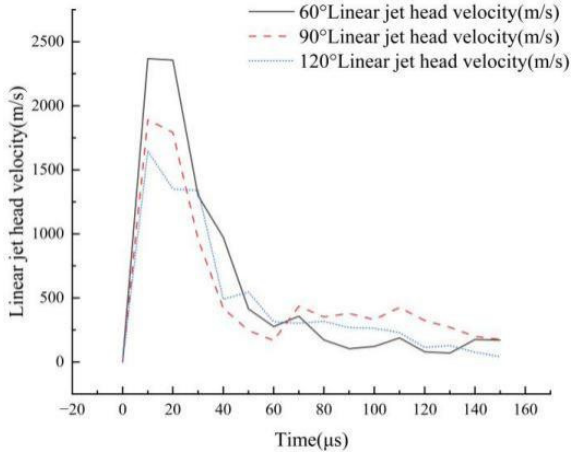


Fig. 6. Velocity-time fitting curves of shaped charge jet heads under different cone angles.

4 Conclusion

Based on the results and discussions presented above, the conclusions are obtained as below:

(1) The linear shaped charge jet perforation structure designed in this study demonstrates effective functionality against rubber targets. For the three conical angle configurations investigated, all achieve optimal damage to rubber targets, indicating that this linear shaped charge jet perforation system is capable of effectively disabling automotive tires, thereby depriving vehicles of mobility.

(2) The liner angle exhibits significant regular characteristics in influencing the penetration behavior of shaped charge jets into rubber targets. As the liner angle increases, the extent of rubber target damage becomes more pronounced, while the time of jet impact on the rubber target is delayed.

(3) During the formation stage of the shaped charge jet, the head velocity of the jet rapidly reaches its maximum value within 10 microseconds. In the subsequent velocity decline phase, distinct velocity distribution characteristics emerge due to variations in the formation and fracture modes of different slug structures. Furthermore, during the jet growth phase, the maximum head velocity exhibits an inversely proportional relationship with the liner conical angle, progressively decreasing as the conical angle increases.

Acknowledgments

This work was financially supported by the Basic Research Project of the Ministry of Public Security's Technical Research Program (2023JSYJC27), the Central Universities Fundamental Research Foundation of China (LGZD202301), Jiangsu Province's

"333 High-level Talent Training Project" and Jiangsu Province Key Discipline "Public Security Technology" during the 14th Five Year Plan (Su Jiao Yan Han [2022] No. 2)

References

1. Yao X, OuYang K F, Gao C and Gao F (2022) Development and test of an assembled modular vehicle barrier. *Protec. Eng.*, 44(1): 16-21. (in Chinese)
2. Brown J, Curtis J P and Cook D D (1992) The formation of jets from shaped charges in the presence of asymmetry. *J. Appl. Phys.*, 72(6): 2136-2143.
3. Meister F J and Haller F (2001) Experimental and numerical studies of annular projectile charges. *Proc. 19th Int. Symp. Ballistics.*, Interlaken, Switzerland, 1: 575-581.
4. Wolfgang S (1994) Modified SDM model for the calculation of shaped charge hole profiles. *Propell. Explos. Pyrot.*, 19(4):192-201.
5. Held M (1996) Initiation criteria of high explosives at different projectile or jet densities. *Propell. Explos. Pyrot.*, 21(5):235-237.
6. Xu W, Wang C and Chen D (2019) The jet formation and penetration capability of hypervelocity shaped charges. *Int. J. Impact Eng.*, 132: 103337.
7. Svirsky O V, Kovalev N P and Klopov B A (2001) The shaped charge jet interaction with finite thickness targets. *Int. J. Impact Eng.*, 26: 735-744.
8. Chen J Y, Feng D L and Sun Q Y (2023) Numerical modeling of shaped charge jet penetration into ceramic metal double-layered medium using smoothed particle hydrodynamics. *Int. J. Impact Eng.*, 175: 104526.
9. Luo D J, Wang Y W and WANG F C (2020) The influence of metal cover plates on ballistic performance of silicon carbide subjected to large scale tungsten projectile. *Mater. Design.*, 191: 108659.
10. Jiang A B, Li Y Q and Li D (2022) Study on anti-penetration performance of semi-cylindrical ceramic composite armor against 12.7 mm API projectile. *CRYSTALS*, 12(10): 1343.
11. Xie X B, Zhong M S, Song G, Ji C and Wu J Y (2018) Effect of inner and outburst height on penetration properties of linear shaped charge cutter under water. *Blast.*, 35(1): 130-136. (in Chinese)
12. Fang Y Z, Zhang X F, Xiong W, Feng K H, Liu C and Ge X L (2023) Study on penetration law of shaped charge jet considering shape distribution characteristics. *Trans. Beijing Inst. Technol.*, 43(10): 1047-1058. (in Chinese)
13. Zhou N, Wang J X and Jiang D K (2020) Study on the failure mode of a sandwich composite structure under the combined actions of explosion shock wave and fragments. *Mater. Design.*, 196(109166): 1-15.
14. Kong X S, Wu W G and Li J (2013) A numerical investigation on explosive fragmentation of metal casing using Smoothed Particle Hydrodynamic method. *Mater. Design.*, 51: 729-741.

Open Access This chapter is licensed under the terms of the Creative Commons Attribution-NonCommercial 4.0 International License (<http://creativecommons.org/licenses/by-nc/4.0/>), which permits any noncommercial use, sharing, adaptation, distribution and reproduction in any medium or format, as long as you give appropriate credit to the original author(s) and the source, provide a link to the Creative Commons license and indicate if changes were made.

The images or other third party material in this chapter are included in the chapter's Creative Commons license, unless indicated otherwise in a credit line to the material. If material is not included in the chapter's Creative Commons license and your intended use is not permitted by statutory regulation or exceeds the permitted use, you will need to obtain permission directly from the copyright holder.

